

## OBSERVATION OF PHOTOLUMINESCENCE FROM MAGNETO-PLASMAS UNDER INTENSE FEMTOSECOND EXCITATION IN STRONG MAGNETIC FIELDS

Y. D. JHO, X. WANG, G. D. SANDERS, D. H. REITZE and C. J. STANTON

*Department of Physics, University of Florida, Gainesville, FL 32611, USA*  
*ydjho@magnet.fsu.edu*

J. KONO

*Department of Electrical and Computer Engineering, Rice University,*  
*Houston, TX 77005, USA*

X. WEI

*NHMFL, Florida State University, Tallahassee, FL 32310, USA*

G. S. SOLOMON

*Solid-State Laboratories, Stanford University, Stanford, California 94305, USA*

We report results on measurements of magneto-photoluminescence at 4.2 K in  $\text{In}_x\text{Ga}_{1-x}\text{As}$  multiple quantum wells in high magnetic fields (25 Tesla) and laser intensities ( $25 \text{ GW/cm}^2$ ) using 150 fs pulses. Novel magneto-plasma phenomena are observed, including strikingly narrow emission lines of Landau levels above a threshold intensity and the suppression of exciton-mixing-induced anti-crossings.

*Keywords:* Magneto-plasma; photoluminescence; magneto-exciton.

### 1. Introduction

The use of strong laser fields to explore quantum optical phenomena has played a major role in our understanding of the interaction of light with atomic systems. Extensive investigations on quantum optical analogs in condensed matter and mesoscopic systems have followed.<sup>1</sup> Nevertheless, a variety of well-known strong field quantum optical phenomena remain for the most part unexplored in condensed matter systems because they require tunable ultrafast lasers to create solid state ‘atoms’ (excitons) and probe them on time scales faster than decoherence times (typically ps or less), in combination with high magnetic fields to freeze the motion of ‘atoms’ and controllably tune their energy levels. Heretofore, the scarcity of tunable ultrafast spectroscopic capabilities at high magnetic field facilities has limited progress in this area. To enable these investigations, we have recently developed an ultrafast spectroscopy laboratory at the DC High Field Facility of the

National High Magnetic Field Laboratory, with the capability of probing over 200 nm - 20  $\mu$ m wavelengths range with 150 fs temporal resolution in fields up to 25 T. As a prelude to investigations of strong field magneto-quantum optics, here we investigate the transition from a magneto-exciton state to a magneto-plasma state in  $\text{In}_x\text{Ga}_{1-x}\text{As}$  quantum wells.

Electron-hole (e-h) plasmas exhibit strong Coulomb correlations at low temperatures in high magnetic fields. For example, band gap renormalization (BGR),<sup>2</sup> carrier effective mass renormalization,<sup>3,4</sup> and spin-splitting effects<sup>5</sup> have been investigated in  $\text{In}_x\text{Ga}_{1-x}\text{As}$  and GaAs quantum wells (QWs) using continuous wave (CW) and nanosecond pulse excitations at relatively low laser intensities. In this paper, by using intense femtosecond pulses, we report our results of magneto-photoluminescence (MPL) in  $\text{In}_x\text{Ga}_{1-x}\text{As}$  QW in high magnetic fields and compare these with low power cw absorption and cw MPL. In particular, we observe the disappearance of exciton coupling and novel MPL emission features from higher-lying Landau levels.

## 2. Experimental Methods

Samples were grown by molecular-beam epitaxy on GaAs substrates. They consist of a GaAs buffer layer grown at 570° followed by 15 layers of 8 nm  $\text{In}_{0.2}\text{Ga}_{0.8}\text{As}$  QW separated by 15 nm GaAs barriers and GaAs capping layer, all grown at a substrate temperature varying between 390-435 ° C. Compressive interface strain induces a large heavy-hole–light-hole(HH–LH) splitting, permitting unambiguous measurements of the HH exciton. For high intensity MPL and time-resolved experiments, we use a 150 fs, 775 nm Clark-MXR Ti:Sapphire chirped pulse amplifier (CPA) to perform measurements as a function of laser power and magnetic field up to 25 GW/cm<sup>2</sup> (fluence of 15 mJ/cm<sup>2</sup>) and 25 T. For near and mid-infrared excitation, the laser pulse seeded an optical parametric amplifier (OPA). A laser power of 8 GW/cm<sup>2</sup> is estimated to generate a carrier density of  $2.4 \times 10^{12} \text{ cm}^{-2}$  at 775 nm in our structure. The excitation beam is delivered to the sample through free space into a 25 T Bitter magnet and MPL is collected by a multi-mode fiber in a specially designed optical cryostat operating at 4.2 K. For cw measurements, illumination/excitation sources and signal collection were performed via multi-mode fiber coupling into and out of the cryostat containing the sample into a magnet capable of 30 T operation. CW PL spectroscopy was performed using the 632-nm line of an He-Ne laser. White-light from a tungsten-lamp was used for absorption and all excitation and collection was done in the normal incidence to the sample surface.

## 3. Results and Discussion

Figure 1(a) displays a series of representative cw absorption spectra as a function of magnetic field. The zero-field PL peaks labeled  $E_1H_1$ ,  $E_1L_1$ , and  $E_2H_2$  represent the 1s exciton peaks associated with the lowest three allowed interband transitions

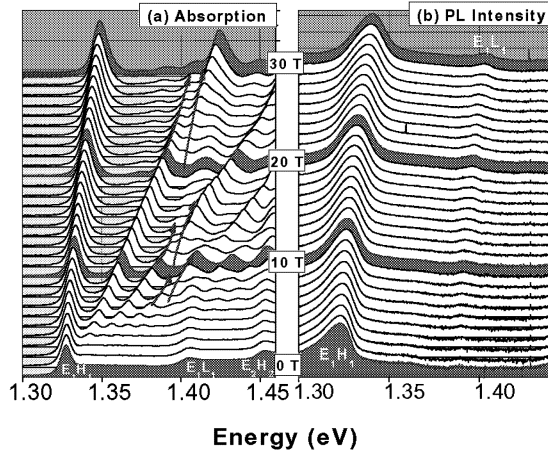


Fig. 1. (a) Absorption and (b) photoluminescence spectra versus magnetic field for  $\text{In}_{0.2}\text{Ga}_{0.8}\text{As}/\text{GaAs}$  multiple quantum wells at 4.2 K. At zero field, three prominent peaks,  $E_1H_1$ ,  $E_1L_1$ , and  $E_2H_2$ , are observed. The arrows highlight the energies where magneto-exciton splitting is seen.

in the quantum well. The splitting between  $E_1H_1$  and  $E_1L_1$  is large ( $\sim 100$  meV) due to the strain. At finite fields, the continuum above each exciton peak splits into Landau levels (or excited magneto-exciton states). In this article, we use the high-field notation, where each state is specified by the electron and hole Landau index  $(N, M)$ ,<sup>6</sup> appropriate for the high-density, plasmonic situation; we also neglect the center-of-mass momentum  $K$  of the electron-hole pairs. Therefore, the lowest three allowed transitions are labelled  $E_1H_1^{00}$ ,  $E_1H_1^{11}$ , and  $E_1H_1^{22}$ . Each excited state shows anti-crossing-like splitting (indicated by arrows) whenever it meets a dark state (assigned to be the  $E_1H_3^{00}$ ) via comparison with 8-band effective-mass calculation.<sup>7</sup> This splitting behavior is independent of polarization, and sensitive only to the parity of the quantum confined states. We attribute the origin of the splitting to excitonic Coulomb interaction.<sup>7</sup> For comparative purposes, figure 1(b) shows cw MPL spectra. Only two peaks ( $E_1H_1$  and  $E_1L_1$ ) are observed.

In contrast, the MPL spectra obtained using femtosecond pulse excitation in Fig. 2 show well defined higher LL states (up to  $E_1H_1^{77}$ ) as reported in previous studies.<sup>3,4</sup> In addition, interestingly, the anti-crossing behavior seen in cw absorption [Fig. 1(a)] appears to be absent. The absence of mixing behavior suggests that prominent PL peaks in Fig. 2 are not purely excitonic, since at high densities the Coulomb interaction should be screened. In Fig. 3, we plot the MPL as a function of excitation intensities for wavelengths (a)  $1.3 \mu\text{m}$ , (b)  $1.1 \mu\text{m}$ , and (c)  $775 \text{ nm}$  at 25 T. For each wavelength, we denote the lowest and highest excitation intensity in  $\text{GW}/\text{cm}^2$  by arrows. Each peak is assigned, from low energy side, to  $E_1H_1^{00}$ ,  $E_1H_1^{11}$ ,  $E_1H_1^{22}$ , and  $E_2H_2^{00}$ , respectively. Excitation at  $1.3$  and  $1.1 \mu\text{m}$  wavelengths is below the QW

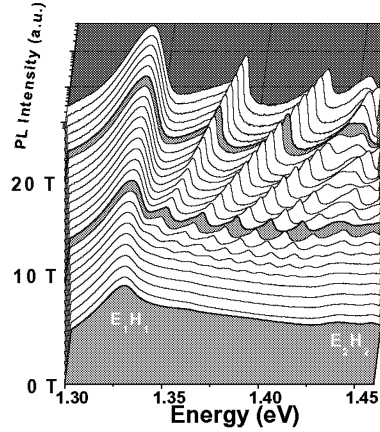


Fig. 2. Magnetic field dependence of photoluminescence from 4.2 K  $\text{In}_{0.2}\text{Ga}_{0.8}\text{As}/\text{GaAs}$  excited by 775 nm, 150 fs, 25  $\text{GW}/\text{cm}^2$  radiation.

band edge, hence, the corresponding MPL is due to two-photon absorption into the GaAs barrier and GaAs capping layer and the continuum states of the QW layer. In contrast, 775 nm light directly excites the barrier, capping layer, and the QW continuum. In both cases, PL emission occurs after carrier relaxation down to the QW subbands. Note that the energy position of each peak in Fig. 3 is shifted relative to that of cw absorption as shown in Fig. 1 due to renormalization of the effective mass. At all excitation densities in Fig. 3(a), the peak energies remain at fixed positions, showing almost no shift against pumping and indicating the suppression of BGR at low excitation power.

With (a) 1.3  $\mu\text{m}$  and (b) 1.1  $\mu\text{m}$  excitation, we observe that the emission of  $E_1H_1^{11}$  and above increase with increasing power, while all LL's are prominent over the whole range in (c) 775 nm. Strikingly, the higher energy peaks  $E_1H_1^{11}$  and  $E_1H_1^{22}$  at high laser intensities have a significantly different character than the  $E_1H_1^{00}$  peak. At a low excitation power in Fig. 3(b) and (c), broad and weak  $E_1H_1^{11}$  and  $E_1H_1^{22}$  peaks appear above the  $E_1H_1^{00}$  peak. With increasing excitation powers, narrow peaks appear on the high-energy side of these peaks, and become dominant at high excitation power. The linewidth of higher energy side peak of  $E_1H_1^{11}$  is 2.3 meV, in clear contrast to that of  $E_1H_1^{00}$  ( $\sim 9$  meV), implying a different origin. Normally, higher lying LL's (or magneto-exciton states) have shorter lifetimes and thus broader lines. In addition, the cw magneto-absorption data as shown in Fig. 1(a) does not show narrow peaks.

To determine how the MPL peak scales with pump power, we analyzed the integrated intensity of  $E_1H_1^{00}$ ,  $E_1H_1^{11}$  low energy tail, and  $E_1H_1^{11}$  high-energy peak (Fig. 3 (d)-(f)). At 775 nm, the PL intensities from all three states rise up very rapidly at pump powers  $< 2 \text{ GW}/\text{cm}^2$  and then saturate. At 1.1  $\mu\text{m}$  and 1.3  $\mu\text{m}$  (Fig. 3(d) and (e)), the integrated  $E_1H_1^{00}$  and low energy tail of  $E_1H_1^{11}$  PL vs pump

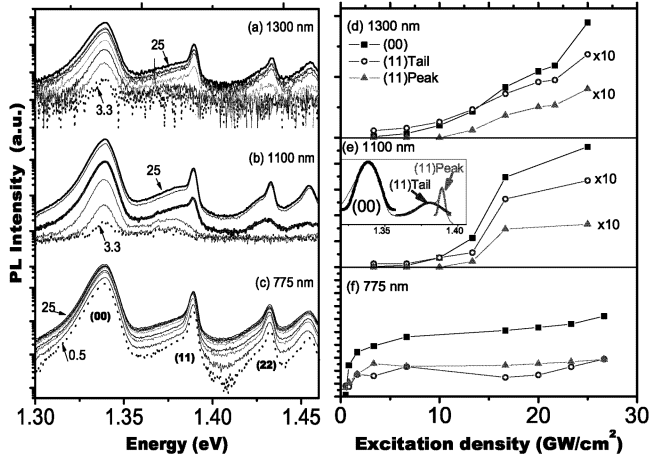


Fig. 3. Pump intensity dependence of photoluminescence obtained at 25 T and 4.2 K using (a) 1.3  $\mu\text{m}$ , (b) 1.1  $\mu\text{m}$ , and (c) 775 nm, 150 fs pulses. (NM) in figure window indicates  $E_1H_1^{NM}$  peak. Integrated photoluminescence intensity for the  $E_1H_1^{00}$  peak (square), low energy  $E_1H_1^{11}$  peak (circle), and high energy  $E_1H_1^{11}$  peak (triangle) for (d) 1.3  $\mu\text{m}$ , (e) 1.1  $\mu\text{m}$ , and (f) 775 nm excitation, respectively. The numbers in (a) through (c) indicate the excitation intensity in  $\text{GW}/\text{cm}^2$ . Inset figure in (e) indicates the specification of each peak used for fitting results.

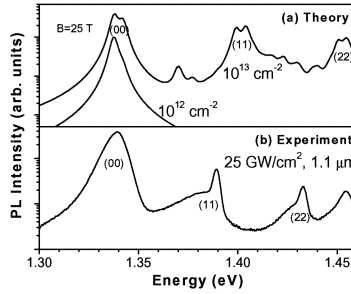


Fig. 4. (a) Theoretical MPL spectra for carrier densities of  $10^{13} \text{ cm}^{-2}$  and  $10^{12} \text{ cm}^{-2}$ . The magnetic field and temperature were fixed at 25 T and 4.2 K. For comparison, experimental MPL spectra obtained with  $25 \text{ GW}/\text{cm}^2$  excitation at 1.1  $\mu\text{m}$  is plotted. (NM) in figure window indicates  $E_1H_1^{NM}$  peak.

power ( $I_{\text{pump}}$ ) scales as  $I_{\text{pump}}^2$ , characteristic of two photon absorption. However, the integrated MPL energy of the narrow peaks display a different scaling. This is particularly evident for the  $E_1H_1^{11}$  peak in Fig. 3(d), which shows no emission until a threshold pump intensity ( $\sim 13 \text{ GW}/\text{cm}^2$ ) and then linearly increases, reminiscent of a stimulated process.

Confirmation that many-body effects play a significant role in femtosecond ex-

cited MPL comes from Fig. 4 (a), which plots the magnetic field-dependent spontaneous emission using an 8 band Pidgeon Brown effective mass model. By comparing the two curves in Fig 4(a) with Figure 4(b), we estimate that the actual carrier density is between  $10^{12} \text{ cm}^{-2}$  and  $10^{13} \text{ cm}^{-2}$  in our experiments. However, discrepancies between theory and experiment appear in the theoretically predicted and experimentally observed energy separations of higher lying MPL peaks, due to the absence of Coulomb interactions and thus renormalization effects in the theory. Spin-splitting was not observed experimentally due to the large inhomogeneous broadening. Significantly, the emergence and power scaling of the narrow emission peaks at the  $E_1H_1^{11}$  and higher LLs seen in the experimental spectra are not observed theoretically. Therefore, we suggest that the experimental curves are influenced by 1) Coulomb correlation effects between dense carriers, particularly with regard to energy and 2) cooperative emission processes at higher lying LLs.<sup>8</sup> More systematic studies are needed to elucidate the origin of these phenomena.

#### 4. Conclusion

We have performed magneto-photoluminescence measurements in  $\text{In}_x\text{Ga}_{1-x}\text{As}$  multiple quantum wells in high magnetic fields using intense femtosecond pulses. Based on the independence of transition energies with increasing power and the absence of mixing behavior, our transition levels are interpreted to be mostly plasmonic. In addition, surprisingly narrow emission lines are seen from higher lying Landau levels, in contrast with the normal high density line broadening expected from magneto-plasmas. Further studies in the temporal and spectral domains are ongoing to elucidate the exact origin of these effects.

#### Acknowledgements

This work was supported by DARPA through Grant No. MDA972-00-1-0034, the NSF ITR program through grant DMR-032547 and the NHMFL In-house Science Program.

#### References

1. Y. Yamamoto and A. Imamoglu, *Mesoscopic Quantum Optics*, (John Wiley & Sons, New York, 1999).
2. G. Tränkle et al., *Phys. Rev. Lett.* **58**, 419 (1987).
3. L.V. Butov et al., *Phys. Rev.* **B44**, 10680 (1991).
4. M. Potemski et al., *Solid State Comm.* **75**, 185 (1990).
5. L.V. Butov et al., *Phys. Rev.* **B48**, 17933 (1993).
6. A.H. MacDonald and D.S. Ritchie, *Phys. Rev.* **B33**, 8336 (1993).
7. Y.D. Jho et al., *unpublished*.
8. A.A. Belyanin et al., *Quantum Semiclass. Opt.* **9**, 1 (1997).